

Nanotechnology E-Newsletter

June 2005

Templated fabrication of non-spherical gold nanoparticles

Extensive research interest in nanometer-dimensioned inorganic particles and clusters has mainly been driven by their broad impact on the emerging disciplines of nanoengineering, nanoelectronics, and nanobioelectronics. Metal nanoparticles—gold in particular—have been the focus of numerous investigations in recent years because of potential optical, electronic, and chemical properties, and their promise in applications such as biosensing.¹⁻³ Of particular interest is the utility of their behaviors due to quantum-confinement effects, with nanocluster-based devices being envisioned as the next generation in electronics miniaturization.

One of the technological challenges is to fabricate robust and organized assemblies of these nanoscale building blocks where the collective structural properties and functions might be manipulated by the size, shape, orientation, and position relative to each other as well as the composition of the nanoparticles. Self-assembled monolayers (SAMs) have attracted special attention because their preparation is simple and the resultant films are densely packed, highly ordered, and largely free of defects. Here, we describe how self-assembled monolayers of alkanedithiol and silane thiol—on metal and glass substrates, respectively—are being used as templates for the nucleation and growth of nano-sized gold particles.⁴

Several methods for the preparation of gold nanoparticles have been investigated: these include the use of colloidal methods, physical vapor deposition process, and template synthe-

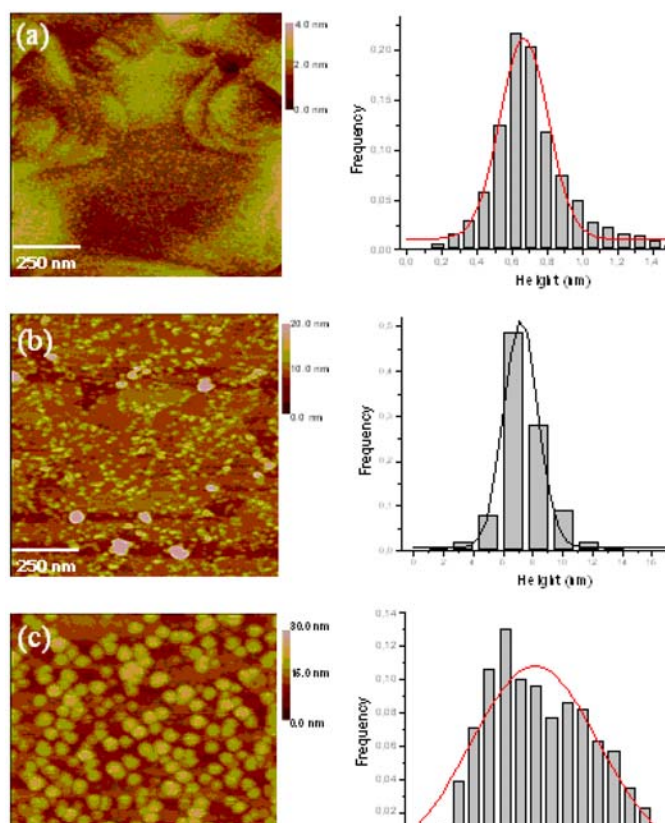


Figure 1. Atomic force microscope (AFM) images of organometallic chemical vapor deposition (OMCVD) gold on SH-terminated self-assembled monolayers (SAMs) on different substrates: (a) 1,8-octanedithiol (C8-DT) SAMs on Au(111); (b) C8-DT SAMs on flat Ag; and (c) 3-mercaptopropyltrimethoxysilane (MPS) SAMs on silicon wafer. On the right of the images are the corresponding height distributions of the gold nanoparticles.

sis. Among the existing methods, the colloidal approach is one of the most popular. However, although large bodies of works have successfully demonstrated that such methods can produce well-defined nanoparticles, there are still some drawbacks. In particular, the stability of

both the particle and the particle's attachment to the surface are at issue, as is controlled aggregation and flexibility for further functionalization. One thing we do know: although nanoparticle superstructures already provide exciting prospects for chemists, physicists, biologists, and material scientists from theoretical, experimental, and practical perspectives, they are still in their infancy. Electronic miniaturization may be eventually be achieved through one of several different paths.

Here we present an alternative method for the preparation of non-spherical gold nanoparticles, all aligned identically with respect to the surface. They are prepared via an organometallic chemical vapor deposition (OMCVD) process where the particles grow attached directly to the template surface. The OMCVD process offers several advantages in addition to the possibility of area-selective deposition where nucleation and growth only occur on so-called growth areas.^{5,6} For instance, the process is economical: deposition is performed under low vacuum and low temperature. Also, the aggregation state of the particles can be controlled because the particles are immobilized on the surface and fixed in their morphology. In addition, using OMCVD, the gold nanoparticles are free and flexible for further functionalization since they are not capped.

To enhance the design and optimization of applications based on OMCVD-fabricated gold nanoparticles, a thorough understanding of their basic properties is necessary. Non-spherical particles—which should exhibit more interesting and exciting

Continues on page 2.

Templated fabrication of non-spherical gold nanoparticles

Continued from cover

plasmon resonance patterns than their spherical counterparts—are presented here. The size and form characterization of OMCVD-grown gold nanoparticles is determined using atomic force microscopy (AFM), scanning tunnelling microscopy (STM), and scanning electron microscopy (SEM). Here, 1,8-octanedithiol (C8-DT) SAMs were used: i) mica substrates carrying a thin layer of gold with (111) orientation on the surface; ii) flat silver substrates; and, iii) 3-mercaptopropyltrimethoxysilane (MPS) on silicon wafers. The precursor for the OMCVD process used is $[(\text{CH}_3)_3\text{P}]\text{AuCH}_3$. The chosen deposition time was 30 minutes.

Figure 1 shows the AFM images of OMCVD gold deposited on: a) C8-DT SAMs on Au(111); b) on flat Ag; and c) on MPS SAMs. A first glance at their height histogram, the particle distribution after deposition both on MPS and on C8-DT SAMs on Ag is more or less the same, with a mean height value of about 7.5nm. The height of OMCVD gold on C8-DT SAMs on Au was remarkably low, with a mean height value of 0.7nm. On the other hand, OMCVD gold nanoparticles on MPS SAMs have the broadest height distribution: its lateral size was the largest of the three samples.

The true lateral sizes were examined via STM and SEM. Figure 2a shows the STM image of the gold nanoparticles from Figure 1a—the C8-DT on (111) Au—and Figure 2b an SEM image of the nanoparticles on MPS. In the case of C8-DT on Au, the average particle height was approximately 0.5nm (obtained via AFM measurements, see Figure 1a) and lateral diameter was about 5nm (from STM measurements, see Figure 2a). Thus, an aspect ratio of 1:10 was found. The other two cases yielded lateral sizes of 7nm (Ag substrate) and 12nm (MPS on silicon). Non-spherical particles showing pancake-like structures with different aspect ratios were fabricated.

One reason why this shape difference occurs is the difference in the orientation of the SAMs relative to the surface: normal for MPS SAMs and the C8-DT SAMs on Ag, and 30° from normal for C8-DT SAMs on Au.⁷ Other reasons can be the surface roughness and the availability of free SH groups.

Figure 3 shows the schematic representation of the non-spherical, pancake-shaped OMCVD gold nanoparticles on MPS SAMs (Figure 10a, aspect ratio 7:10=0.6), the C8-DT SAMs on Au(111) (Figure 10b, aspect ratio 1:10=0.1), and the C8-DT SAMs on Ag (Figure 10c, aspect ratio 7:10=0.7).

In future, nanoscale lateral structuring of the template SAMs into growth and non-growth regions will be performed using modern meth-

ods such as electron-beam or focused-ion-beam lithography. This will allow for OMCVD gold nanoparticle arrays with various symmetries.

The authors would like to acknowledge the Federal Ministry of Education and Research (Germany) and its Center for Multifunctional Materials, the German Research Association, and the Academic Development Fund of the University of Western Ontario, for financial support.

Anne Kathrena A. Aliganga,
and Silvia Mittler

Department of Physics and Astronomy
The University of Western Ontario, Canada
E-mail: smittler@uwo.ca

References

1. U. Kreibitz and V. Vollmer, **Optical Properties of Metal Clusters**, Springer, Berlin, 1995.
2. C. Bohren and D. Huffmann, **Absorption and Scattering of Light by Small Particles**, Wiley, New York, 1998.
3. Z.Y. Zhong, K.B. Male, and J.H.T. Luong, *More recent progress in the preparation of Au nanostructures, properties, and applications*, **Analytical Lett.** **36** (15), p 3097, 2003.
4. A. Ulman, **An introduction to ultrathin organic films: from Langmuir-Blodgett to self-assembly**, Academic Press, Boston 1991.
5. P. Wohlfart, J. Weiß, J. Käshammer, C. Winter, C. V. Scheumann, R.A. Fischer, and S. Mittler-Neher, *Selective ultrathin gold deposition by organometallic chemical vapor deposition onto organic self-assembled monolayers (SAMs)*, **Thin Solid Films** **340**, p. 274, 1999.
6. C. Winter, U. Weckenmann, R.A. Fischer, J. Käshammer, V. Scheumann, and S. Mittler, *Selective nucleation and area selective OMCVD of gold on patterned self-assembled organic monolayers studied by AFM and XPS: a comparison of OMCVD and PVD*, **Advanced Materials: CVD** **6**, p. 199, 2000.
7. A. Ulman, *Formation and structure of self-assembled monolayers*, **Chem. Rev.** **96**, p. 1533, 1996.

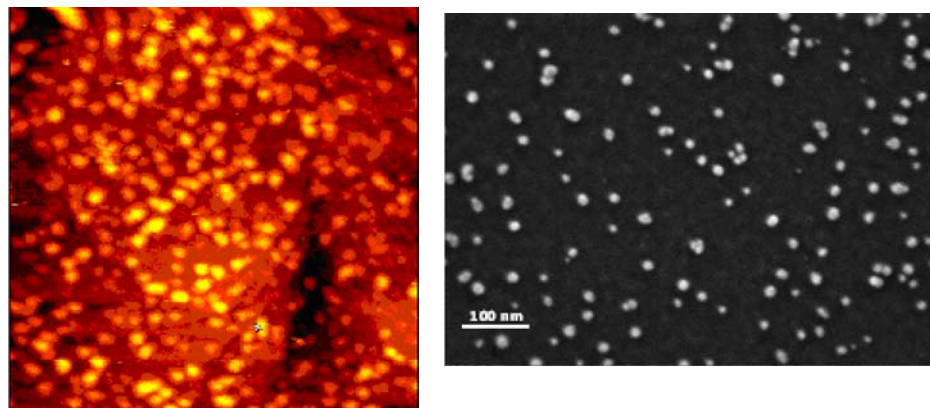


Figure 2. (a) Scanning tunnelling microscope (STM, 195nm×195nm) image of organometallic chemical vapor deposition (OMCVD) gold nanoparticles on 1,8-octanedithiol (C8-DT) self-assembled monolayers (SAMs) on Au(111) substrate. (b) scanning electron microscope (SEM) images of OMCVD gold on 3-mercaptopropyltrimethoxysilane (MPS).

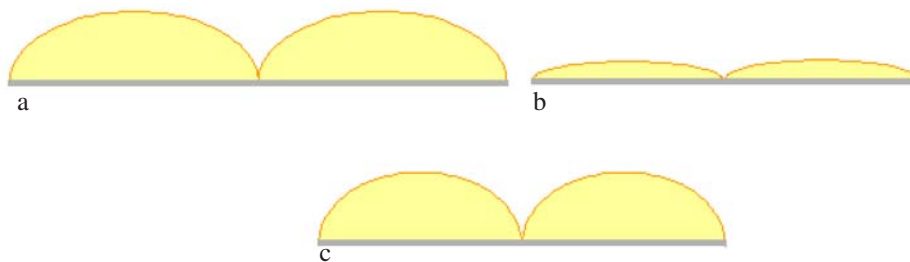


Figure 3. Schematic illustration of the non-spherical OMCVD gold nanoparticles grown on: (a) MPS SAMs (8nm height, 12nm lateral size); (b) on C8-DT SAMs on Au(111) (0.5nm height, 5nm lateral size); and (c) on C8-DT SAMs on Ag (7nm height, 10nm lateral size).

Detecting and controlling a single electron in quantum dots using an atomic force microscope

Quantum dots (QDs) of various kinds are among the most important devices in nanotechnology. A variety of applications of the technology are being pursued, including information storage, improvement in laser efficiency, and quantum computation. Although detection and control of the charging state of individual QDs is considered to be a key technique for those applications, it still remains challenging—especially for self-assembled semiconductor quantum dots and nanoparticles—due to the difficulty of attaching leads to such small nano-objects.

We have developed a new technique to address this issue based on the detection of electrostatic force by an atomic force microscope (AFM). It enables us to detect and control the charging state of individual QDs using a single-electron charge. An AFM probe serves as an electrometer for charge detection as well as a gate electrode for modulating the charge. The long-range nature of electrostatic force enables the detection of the charging state of the QD with relatively large distance between the tip and quantum dot, and the quantum-dot and substrate. This means that the technique is applicable even to capped QDs, which are practically more important, as no current has to be collected at the tip. Moreover, in light of potential qubit readout by AFM for quantum computation, the ability to detect the charging state of the quantum dot weakly coupled to external leads is of great importance, since a strong coupling introduces decoherence of the qubit. In particular, single-shot measurements of individual electronic charge are a necessary condition and could be achieved by a weak capacitive coupling between the

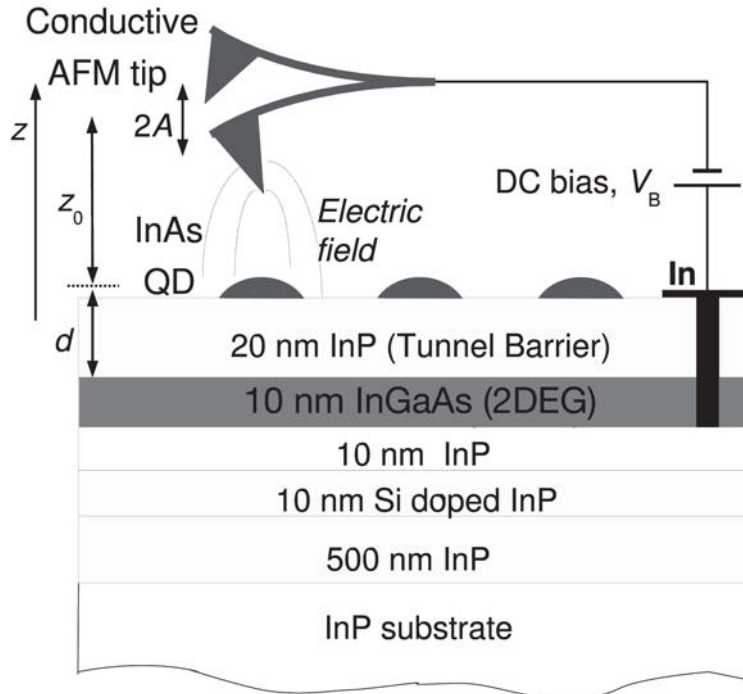


Figure 1. Schematic diagram of the sample quantum-dot structure and the experimental setup to detect the electronic charge.

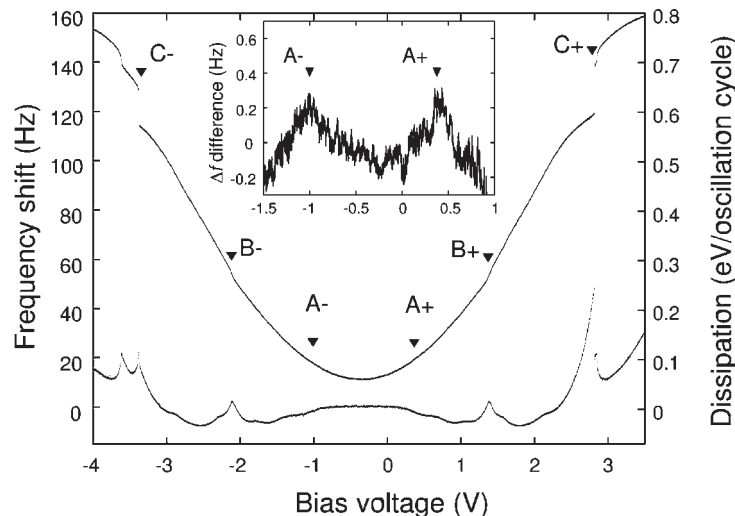


Figure 2. Shown is the resonance-frequency shift and dissipated energy of the atomic force microscope (AFM) cantilever as a function of the tip-back electrode voltage. The jumps and peaks indicated by arrows in each curve correspond to single-electron charging events in a single InAs quantum dot.

charge detector (AFM tip in our case) and the dot.

Figure 1 depicts the sample structure and the experimental setup. Self-assembled InAs QDs are grown onto InP substrate by chemical-beam epitaxy. A two-dimensional electron gas (2DEG) formed in the InGaAs quantum well was used as the back electrode, sitting 20nm underneath a layer of InAs quantum dots. An InP spacer layer between the QD layer and the 2DEG layer serves as a tunneling barrier. An oscillating conductive AFM tip is brought above a single InAs quantum dot (at 4.5K, in vacuum) with a typical average tip-QD distance of 20nm. The resonance-frequency shift and dissipated energy of the oscillating cantilever are measured as a function of the tip-back-electrode bias voltage. These two quantities are measures of the electrostatic force and the energy dissipated in the sample.

Figure 2 depicts the measured results. The resonance-frequency shift shows several jumps on a parabolic background that account for a capacitive interaction between the tip and the back electrode. The jumps can be interpreted by a series of single-electron charging events: a result of single-electron tunneling from the back electrode to the quantum dot. These jumps are essentially measuring the Coulomb blockade energies in the dot. The corresponding structures appear in the dissipation signal as peaks, which are a measure of energy dissipation due to the single-electron tunneling process.

This technique could be used for the investigation of the electronic structure of an individual QD without defining additional leads. In addition, the access to the dissipation signal could enable the investigation of the in-

Continues on page 4.

Detecting and controlling a single electron in quantum dots using an atomic force microscope

Continued from page 3.

triguing interaction between micromechanical oscillators and single-electron systems.

R. Stomp, Y. Miyahara, S. Schaer, Q. Sun, H. Guo, P. Grutter, S. A. Studenikin*, P. Pool*, and A. Sachrajda*

Department of Physics,
McGill University, Montreal, Canada

*Institute for Microstructural Science,
National Research Council of Canada

E-mail: {miyahara,
grutter@physics.mcgill.ca}

Reference

1. R. Stomp, Y. Miyahara, S. Schaer, Q. Sun, H. Guo, S. Studenikin, P. Pool, A. Sachrajda, and P. Grutter, **Phys. Rev. Lett.** **94** 056802, 8 February 2005.

The conceptualization of metamaterials through homogenization

Suppose we consider the electromagnetic response of a composite metamaterial that consists of a random collection of disparate particles. Provided that the linear particulate dimensions are small relative to electromagnetic wavelength(s), the composite may be regarded as being effectively homogeneous. The constitutive parameters of such a homogenized composite medium (HCM) may be estimated using any one of several homogenization formalisms.¹ The process of homogenization has the potential to extend electromagnetic/optical material properties and therefore is of considerable importance in the design of novel materials.

The term metamaterial has been coined to describe artificial composites that exhibit physical properties that are either not at all exhibited by their component phases or not exhibited to the same extent by their component phases. Prime examples of metamaterials are provided by HCMs. In this communication, a brief survey of five different conceptualizations of HCM-based metamaterials is presented. Our focus is on the interesting electromagnetic/optical properties that may be realized rather than the mathematical details of homogenization—further details of the theory are available elsewhere.²

1. In electromagnetics, the most general linear material is called bianisotropic: here, the dielectric displacement \mathbf{D} is anisotropically-coupled to both the electric field \mathbf{E} and the magnetic field \mathbf{H} , and the magnetic induction \mathbf{B} is anisotropically-coupled to both \mathbf{E} and \mathbf{H} . While manifestations of bianisotropy are not readily observed in naturally-occurring materials, bianisotropic HCMs may be readily conceptualized. In order to do this, it is necessary that one of the HCM components is anisotropic and another exhibits magnetoelectric coupling. For example, the homogenization of a biaxial dielectric material with an isotropic chiral material gives rise to a biaxial bianisotropic HCM.²

2. Generally, biaxial dielectric materials exhibit birefringence. That is, there are generally two different wavevectors associated with planewave propagation in a given direction. The wavevectors and wavenumbers arise as

eigenvectors and eigenvalues, respectively, of a 2×2 propagation matrix. Exceptionally, this matrix yields only one independent eigenvector and one eigenvalue: the corresponding plane wave is called a Voigt wave. Such waves exhibit an unusual property: their amplitude is linearly dependent upon propagation distance.

A key characteristic of materials that support Voigt wave propagation is that they are biaxial; i.e., Voigt waves cannot propagate in uniaxial materials. However, two such materials may be homogenized to produce a biaxial HCM, provided that the distinguished axes of the uniaxial components do not coincide. Numerical calculations have revealed that biaxial HCMs may be conceptualized that support Voigt wave propagation, even though their uniaxial component phases do not.³

3. The phase velocity of a plane wave is called negative if it is directed opposite to the rate of energy flow (as provided by the time-averaged Poynting vector). Several unusual properties follow as a consequence of negative phase velocity (NPV), the most notable being negative refraction.⁴ The issue of NPV propagation has recently generated much excitement in the optics/electromagnetics communities, prompted by experimental reports of microwave negative refraction in metamaterials.⁵

The scope for realizing NPV propagation is generally greater in more complex materials, as the parameter space is correspondingly larger. For example, numerical studies have revealed that we may conceptualize a bianisotropic HCM, in the form of a Faraday chiral medium, that supports NPV propagation while its component phases do not. The Faraday chiral medium develops as a result of homogenizing an isotropic chiral medium with a magnetically-biased ferrite.⁶

4. Within the realm of isotropic dielectric materials, let us consider the homogenization of one component phase with relatively-high refractive index and low dispersion with another that has relatively-low refractive index and high dispersion. Using the Bruggeman homogenization formalism, it has been demonstrated that the group velocity in the corresponding HCM can exceed the group velocity in either component phase, for certain ranges

of volume fraction.⁷

5. Finally, we turn to nonlinear materials. By means of homogenization, an enhancement of nonlinear properties may be achieved. For example, if we consider the homogenization of a weakly nonlinear material with one that is linear, then the degree of nonlinearity exhibited by the resulting HCM can exceed that of its component phases for certain ranges of volume fraction. This nonlinearity enhancement has been established for both isotropic⁸ and anisotropic⁹ HCMs.

In conclusion, electromagnetic/optical material properties may be extended in various ways through homogenization. Thus, HCM-based metamaterials have much to offer in the design of new materials.

Tom G. Mackay

School of Mathematics
University of Edinburgh, UK
E-mail: T.Mackay@ed.ac.uk

References

1. A. Lakhtakia (ed.), *Selected Papers on Linear Optical Composite Materials*, SPIE Press, Bellingham, WA, 1996.
2. T. G. Mackay, *Homogenization of linear and nonlinear complex composite materials, Introduction to Complex Mediums for Optics and Electromagnetics*, W. S. Weiglhofer and A. Lakhtakia (eds.), SPIE Press, Bellingham, WA, pp. 317-345, 2003.
3. T. G. Mackay and A. Lakhtakia, *Correlation length facilitates Voigt wave propagation*, *Waves Random Media* **14**, L1-L11, 2004.
4. J. B. Pendry, *Negative refraction*, *Contemp. Phys.* **45**, pp. 191-202, 2004.
5. R. A. Shelby, D. R. Smith, and S. Schultz, *Experimental verification of a negative index of refraction*, *Science* **292**, pp. 77-79, 2001.
6. T. G. Mackay and A. Lakhtakia, *Plane waves with negative phase velocity in Faraday chiral mediums*, *Phys. Rev. E* **69** 026602, 2004.
7. T. G. Mackay and A. Lakhtakia, *Enhanced group velocity in metamaterials*, *J. Phys. A: Math. Gen.* **37**, L19-L24, 2004.
8. T. G. Mackay, A. Lakhtakia, and W. S. Weiglhofer, *Electromagnetic homogenization of cubically nonlinear, isotropic chiral composite mediums via the strong-property-fluctuation theory*, *Electromagnetics* **23**, pp. 455-479, 2003.
9. T. G. Mackay, *Geometrically derived anisotropy in cubically nonlinear dielectric composites*, *J. Phys. D: Appl. Phys.* **36**, pp. 583-591, 2003.

